Proceedings of ISFOG 2025
5TH INTERNATIONAL SYMPOSIUM ON
FRONTIERS IN OFFSHORE GEOTECHNICS
Nantes, France | June 9-13 2025

ISBN 978-2-85782-758-0

Multidirectional perpendicular drained cyclic behaviour of a marine sand

K. Z. Wen*
University of Oxford, Oxford, United Kingdom

R.M. Buckley
University of Glasgow, Glasgow, United Kingdom

B.W. Byrne
University of Oxford, Oxford, United Kingdom

**kathy.wen@spc.ox.ac.uk (corresponding author)*

ABSTRACT: This study investigates the multidirectional perpendicular behaviour of a marine sand using the Variable Dynamic Direct Cyclic Simple Shear (VDDCSS) device. The loading simulates misaligned wind and wave forces, common at certain offshore sites. VDDCSS tests were conducted in drained conditions and at two relative densities (D_r). For comparison a suite of unidirectional only cyclic tests was also completed. Results suggest that the constant stress amplitude ($\zeta_{b,x}$) (sustained load in the x direction) is a critical parameter across all loading regimes for both densities. A higher $\zeta_{b,x}$ increases the cyclic resistance of the soil demonstrated by increasing stiffness with cycles. The cyclic amplitude ($\zeta_{b,y}$) (cyclic load in the y direction) and cyclic asymmetry ($\zeta_{c,y}$) dictate the magnitude and direction of strain, respectively. Furthermore, multidirectional tests demonstrate lower cyclic resistance compared to unidirectional tests through increased accumulated strain (γ_{acc}). The results highlight the importance of accurately modelling multidirectional soil behaviour in the context of offshore foundation design.

Keywords: multidirectional loading, cyclic loading, sand, variable dynamic direct cyclic simple shear tests

1 INTRODUCTION

Offshore foundations are subjected to complex cyclic loading from environmental actions such as wind and waves. Under storm loading conditions, rapid loading rates leads to undrained to partially drained behaviour which can be critical for design (Peralta et al, 2017; Jostad *et al*., 2020). However, under operational conditions in the long-term, slower loading rates lead to drained conditions in cohesionless soils (e.g. Achmus & Song, 2022). Offshore wind turbines (OWTs) additionally face operational processes caused by rotor mass and aerodynamic imbalances, wind shear, and tower shadow effects as blades pass the tower. Consequently, OWTs often experience a high degree of spatial variability in the loading direction. This spatial variability can also result from factors such as coastal geography, atmospheric conditions, and seasonal weather patterns. Thus, the design of foundations in offshore conditions additionally requires consideration of multidirectional loading.

To investigate the effects of multidirectional loading, Le and Rackwitz (2020) performed drained cyclic simple shear tests under multidirectional loading, where the direction of the cyclic load rotates by 90° at least once during cycling. Specimens exposed to changes in direction during cyclic loading developed a significant amount of strain immediately after rotation in the direction of loading, causing a temporary increase in strain rate. A reduction in stiffness was also observed at the onset of rotation in the loading direction. Bhaumik et al. (2023) demonstrate that multidirectional elliptical and Figure-8 cyclic loading induce greater densification than unidirectional cyclic loading. Dry 1g model tests of a monopile founded in Leighton Buzzard Sand (LBS) by Richards et al. (2020) showed that multidirectional perpendicular loading impacts the rate of accumulated strain for the first 100 cycles, however, perpendicular tests converged to the strain of the unidirectional test after 100 cycles. Richards et al. (2020) indicate that strain accumulates in the direction of average stress for T-shaped perpendicular tests and at an angle to the direction of average stress in L-shaped perpendicular tests depending on the cyclic amplitude. For Fan-type loading, the spread angle, Φ_F was shown to control the magnitude of strain.

These studies investigated the difference between unidirectional and multidirectional loading on the cyclic behaviour of sands. However, the underlying physical mechanisms driving these differences, particularly the effects of constant stress and cyclic stress on features such as densification and stiffness evolution under multidirectional loading, remain less well understood. This paper focuses on the effects of perpendicular multidirectional loading, representing misaligned wave and wind forces, on Cuxhaven sand (CX), a marine sand representing that typically found offshore in the North Sea. The impact of cyclic loading applied in one direction with a constant stress applied in the orthogonal direction is assessed against an equivalent set of unidirectional tests. Tests were performed in drained conditions at two relative densities (D_r).

2 CYCLIC DEFINITIONS

In element testing, cyclic loading refers to the repeated application of stress, τ, or strain, γ, to a specimen as defined by the average, τ_{ave}, and cyclic, τ_{cyc}, shear stress, see Figure 1(a). The resultant average, γ_{ave}, and cyclic, γ_{cyc}, shear strain are shown in Figure 1(b). The minimum and maximum shear stress, τ_{max} and τ_{min}, are defined below:

$$\tau_{max} = \tau_{ave} + |\tau_{cyc}| \quad (1)$$

$$\tau_{min} = \tau_{ave} - |\tau_{cyc}| \quad (2)$$

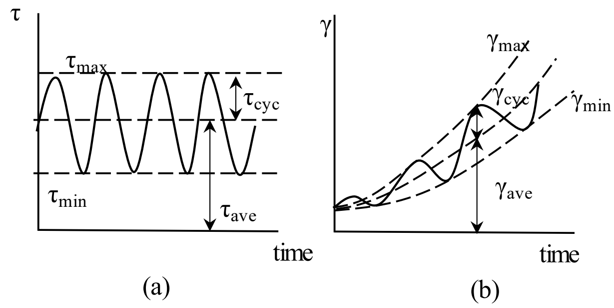

Figure 1 Cyclic definitions (a) τ with time (b) γ with time

The cyclic load amplitude ratio, ζ_b, and loading asymmetry ratio, ζ_c, are defined as:

$$\zeta_b = \frac{\tau_{max}}{\tau_f} \quad (3)$$

$$\zeta_c = \frac{\tau_{min}}{\tau_{max}} \quad (4)$$

Where τ_f is the shear stress from monotonic tests at the relevant density defined as the τ at $\gamma = 15\%$. For multidirectional tests loads are applied orthogonally. In this study, perpendicular multidirectional loading is investigated where the load in the x-direction remains constant $\zeta_{c,x} = 1$ and cyclic loading is applied in the y-direction. Thus, four unique parameters characterise this type of loading: the constant and cyclic load amplitude ratios $\zeta_{b,x}$ and $\zeta_{b,y}$ respectively (as illustrated in Figure 2) and the asymmetry $\zeta_{c,x}$ and $\zeta_{c,y}$ in the x and y direction respectively.

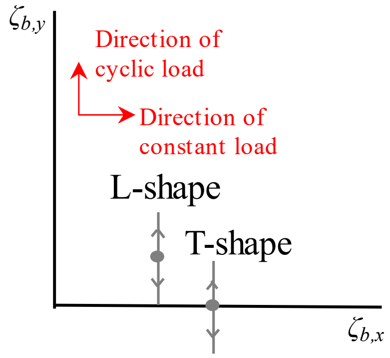

Figure 2 Perpendicular loading (L- and T-shape denotes one-way and two-way loading, respectively)

3 EXPERIMENTAL METHODS

3.1 Materials considered

CX sand is a well-graded, silica sand. The sand is sub-rounded with traces of gravel and silt. The material was obtained via boreholes from the PICASO test site 5 km south of Cuxhaven, Germany, and 6 km east of the North Sea coast; Byrne et al. 2025a. The site is part of an active sand quarry. Table 1 summarises the index properties and Figure 3 presents the particle size distribution

Table 1. Classification properties of investigated sands

d_{50} (mm)	C_u (-)	e_{min}* (-)	e_{max}* (-)	G_s (kg/cm^3)
0.12	2.3	0.44	0.96	2.64

**Determined via NGI method, see Knudsen et al. (2020)*

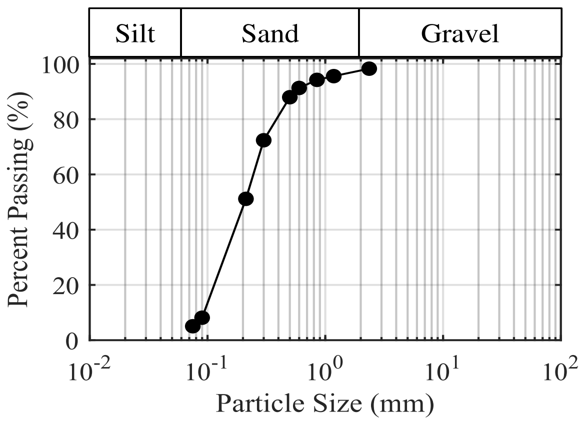

Figure 3 particle size distribution of the tested material

3.2 Testing apparatus

This study utilises the Variable Dynamic Direct Cyclic Simple Shear (VDDCSS) NGI-style apparatus manufactured by GDS Instruments. The VDDCSS is a simple shear device that allows for shearing of the soil specimen in two orthogonal horizontal directions; see Figure 4. A specimen of soil sits within a latex membrane confined by a set of steel rings attached to the load cell by O-rings. A target vertical stress, σ'_v, was applied to the specimen at a rate of 100 kPa per hour until creep strains reduced to < 0.0002 %. This was followed by shearing. In the VDDCSS, drained conditions are induced by allowing volume change to the specimen during shearing whilst keeping σ'_v fixed.

Pertinent cyclic features include accumulated strain, γ_{acc}, which refers to the plastic strains developed in the direction of load bias, the secant shear stiffness, G_{sec}, and energy dissipation η. These features are schematically shown in Figure 5 and described by Equation 5 to 7 below.

$$\gamma_{acc} = \frac{1}{2}(\gamma(a_n) + \gamma(b_n)) \quad (5)$$

$$G_{sec} = \frac{\tau(a_0) - \tau(b_0)}{\gamma(a_0) - \frac{1}{2}(\gamma(b_0) + \gamma(b_1))} \quad (6)$$

$$\eta = \frac{1}{2\pi} \frac{2G_{sec} \oint \tau dy}{(\tau_{cyc})^2} \quad (7)$$

The study also examines changes in relative density, (ΔD_r). Since the cross-sectional area of the specimen is constrained, ΔD_r is directly proportional to changes in axial strain.

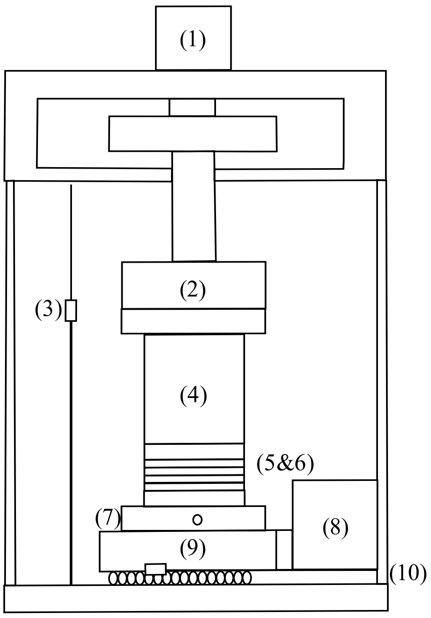

(a)

(1) Vertical actuator
(2) Vertical load cell
(3) Axial LVDT
(4) Top cap
(5) Soil specimen
(6) Confining rings
(7) Base pedestal
(8) Horizontal load cell
(9) Sliding carriage
(10) Horizontal LVDT

Figure 4. VDDCSS Apparatus - Schematic of device

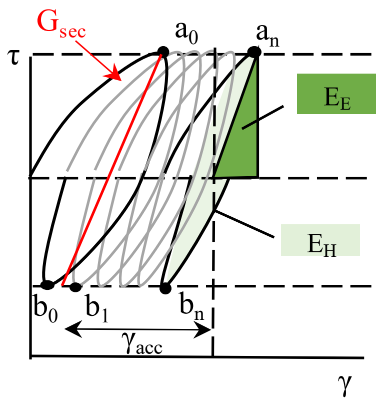

Figure 5. Typical stress strain behaviour

4 RESULTS

4.1 Monotonic results

Monotonic tests were undertaken at constant vertical stress σ'_v = 74 kPa, representative of pile tip stresses from medium-scale field tests (Byrne et al., 2025b), to obtain the reference monotonic strength, τ_f at γ = 15%; see Table 2 and Figure 6. Two D_r were targeted, referred to as 'looser' and 'denser'. A reverse-engineered approach was employed to back-calculate the initial D_r to achieve the desired value prior to shearing. The final D_r inevitably varied, and precise and consistent D_r could not always be ensured across tests.

Table 2. Monotonic test conditions and results.

Test ID*	**D_r (%)****	**σ'_v(kPa)**	**τ_f (kPa)**
M1	70	74	39
M2	100	74	51

**M – monotonic **Approximate densities measured after consolidation*

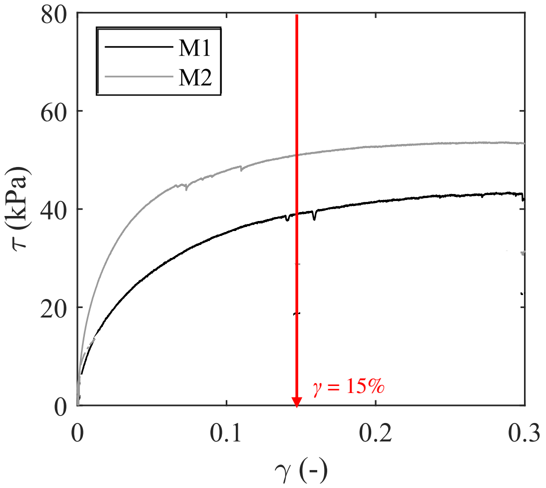

(a)

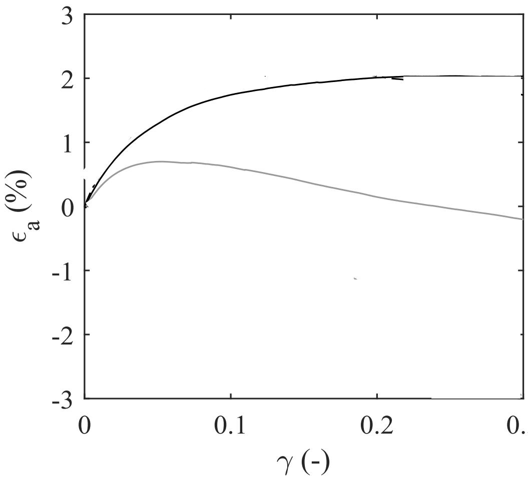

(b)

Figure 6 Monotonic test responses schematically showing the derivation of τ_f (a) Stress-strain (b) Axial strain

The effective friction angle (φ') of the CX sand was between 28 and 34°, lying below typical values observed in similar materials at comparable densities (e.g. Blaker & Andersen, 2015).

4.2 Cyclic results & Discussion

Cyclic tests were conducted at σ'_v = 74 kPa at two target D_r (70-80% and 100%). Loading was applied at a frequency of f = 0.1 Hz for a maximum of 3000 cycles . A failure criterion of γ_{ave} = 15% was adopted. The cyclic parameters are presented in Table 3.

Table 3. Cyclic test conditions and results

Test ID*	D_r [%]	$\zeta_{b,x}$ [-]	$\zeta_{c,x}$ [-]	$\zeta_{b,y}$ [-]	$\zeta_{c,y}$ [-]
UL1	80	0.4	0	0	0
UD1	100	0.4	0	0	0
MDL1	70	0.2	1	0.2	-1
MDL2	70	0.4	1	0.2	-1
MDL3	80	0.4	1	0.6	0.33
MDD1	100	0.2	1	0.2	-1
MDD2	100	0.4	1	0.2	-1
MDD3	90	0.4	1	0.6	0.33

**U – unidirectional, MD – multidirectional, L – loose, D – dense*

The multidirectional strain response in the *x, y* plane for looser and denser specimen are shown in Figure 7 (a) and (b) respectively. The direction of γ depends on $\zeta_{c,y}$. For $\zeta_{c,y}$ = -1 (two-way symmetrical loading), γ accumulates in the direction of $\zeta_{b,x}$. For $\zeta_{c,y}$ > -1, γ accumulates at an angle (θ) to direction of $\zeta_{b,x}$. The value of θ is positively correlated with $\zeta_{b,y}$. These trends are consistent across both the looser and denser specimens; however, the denser specimens accumulate less γ than their looser counterparts. The evolution of ΔD_r, γ_{acc}, G_{sec} and η with cycles for all tests are shown in Figure 8 (a) to (d).

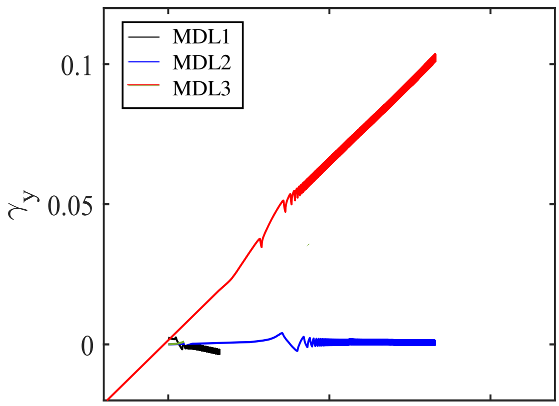

(a)

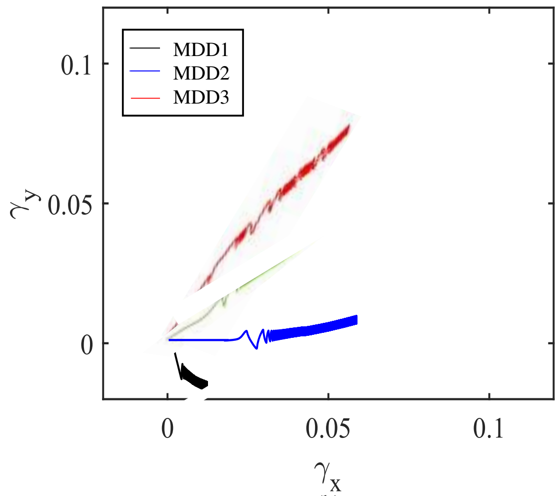

(b)

Figure 7 Multidirectional strain (a) Looser (b) Denser

Across all tests in this study, γ_{ave} did not exceed 15%, and therefore none of the specimens experienced failure within 3000 cycles. All specimens underwent densification due to cycling at similar rates except UD1 which required more cycles before the same level of densification was achieved.

Generally, unidirectional drained tests produced greater changes in ΔD_r and increase in G_{sec} compared to equivalent multidirectional tests. Additionally, unidirectional tests consistently resulted in lower γ_{acc} than multidirectional counterparts. These trends suggest that sands have a greater cyclic resistance under unidirectional cyclic loading as evidenced by the enhanced densification and stiffness increase and reduced strain accumulation.

Within the multidirectional series, $\zeta_{b,x}$ was observed to increase ΔD_r when comparing test pairs with all other parameters held constant (i.e., MDL1 vs MDL2, MDD1 vs MDD2). This trend suggests that higher constant stress levels promote particle re-arrangement and densification.

Figure 7 Cyclic results (a) ΔD_r (b) γ_{acc} (c) $G_{sec}/G_{sec,1}$ (d) η with cycles

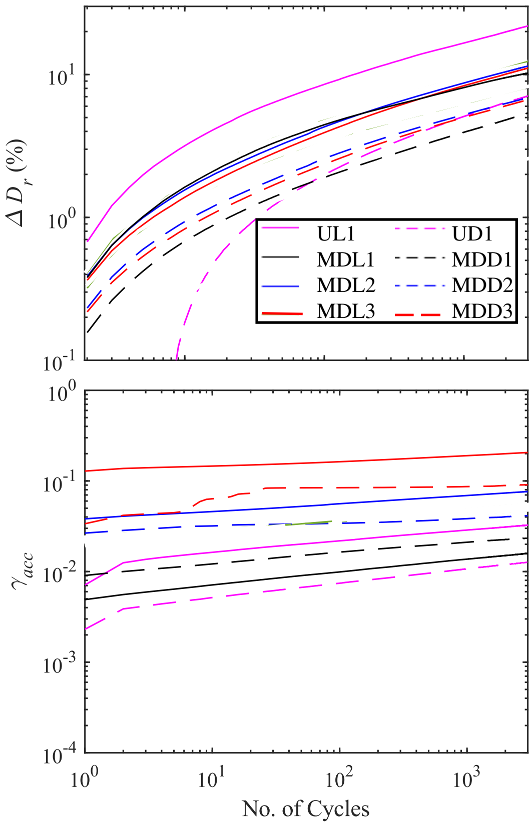

(b)

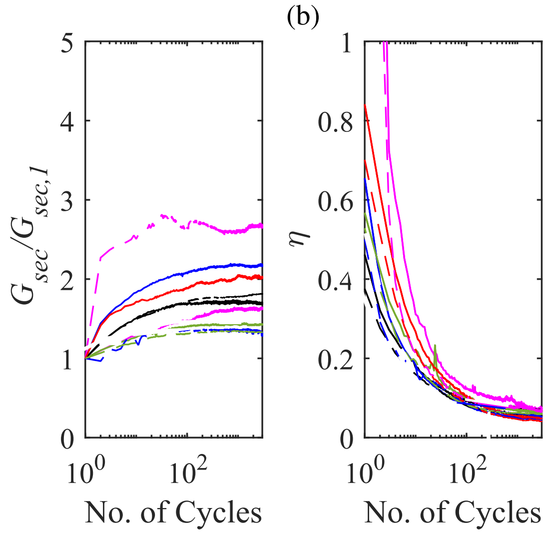

(c) (d)

Similar trends were observed for stiffness evolution. All specimen displayed an increase in G_{sec} with cycling, which is attributed to densification and inter-particle interlocking. Like densification, a positive correlation between $\zeta_{b,x}$ and stiffness increase, $G_{sec}/G_{sec,1}$ was observed, confirming that sands have a greater cyclic resistance under higher sustained values of $\zeta_{b,x}$

Denser specimens exhibited lower ΔD_r and smaller increases in G_{sec} than their looser counterparts. This is likely due to the limited voids which restrict particle rearrangement, densification and stiffness increase.

5 CONCLUSION

Key findings from the study are summarised below. For multi-directional tests under drained cyclic loading conditions:

- $\zeta_{b,x}$ and $\zeta_{c,y}$ control the magnitude and direction of γ_{acc}, respectively.
- γ_{acc} is positively correlated with $\zeta_{b,y}$ and θ is positively correlated with $\zeta_{c,y}$.
- Unidirectional tests obtained higher ΔD_r and stiffness increase than multidirectional tests.
- Unidirectional tests obtained lower γ_{acc} value than multidirectional tests.
- Densification and stiffness increase is positively related to $\zeta_{b,x}$, thought to be due to greater particle rearrangement and interlocking.
- Denser specimens consistently produced lower ΔD_r and lower stiffness increases than looser specimens, attributed to fewer available voids for particle rearrangement.
- γ_{acc} is positively proportional with $\zeta_{c,y}$ across multidirectional tests.

AUTHOR CONTRIBUTION STATEMENT

K. Z. Wen: Laboratory testing, interpretation, formal analysis, writing. **R. M. Buckley**: Supervision, reviewing and editing. **B. W. Byrne**: Supervision, funding acquisition, reviewing and editing.

ACKNOWLEDGEMENTS

The support by Ørsted for the PICASO project is acknowledged. Byrne is supported by the Royal Academy of Engineering under the Research Chairs and Senior Research Fellowships scheme.

REFERENCES

Achmus, M. and Song, J., 2022. Derivation of cyclic py curves for the design of monopiles in sand. In *Current Perspectives and New Directions in Mechanics, Modelling and Design of Structural Systems*. CRC Press.

Bhaumik, L., Rutherford, C. J., Olson, S. M., Hashash, Y. M. A., Numanoglu, O. A., Cerna-Diaz, A., and Weaver, T. J. (2023). A Multidirectional Cyclic Direct Simple Shear Device for Characterizing Dynamic Soil Behavior, *Geotechnical Testing Journal*

Blaker, Ø. and Andersen, K.H., *(2015)* Shear strength of dense to very dense Dogger Bank sand. *International Symposium on Frontiers in Offshore Geotechnics*

Byrne, B. W., Burd, H. J., Kamas, I., Keane, R., Malhorta, S., Martin, S.C., Nardelli, V., Qiu, Z., Rasmussen, M.E., Simonin, L., Saberi, M., Wen, K. Z., Wu., K., Buckley, R. M., Crispin, J. J., Shonberg, A., Cunha, V. L. S., Vaitkune, E (2025a) PICASO: Cyclic loading of wind turbine monopiles, *International Symposium on Frontiers in Offshore Geotechnics*

Byrne, B. W., Buckley, R. M., Burd, H. J., Crispin, J. J., Crook, A., Houlsby, G. T., Keane R., Nardelli, V., Rasmussen, M., Saberi, M., Turner, S., Cunha, V. L. S., Vaitkune, E., Wen, K. Z. (2025b) Cyclic loading of monopiles at a saturated dense sand site in Germany, *International Symposium on Frontiers in Offshore Geotechnics*

Knudsen, S., Powell, J.J.M., Lunne, T., Thomsen, N.V., Krogh, L., and Barwise, A. 2020. Development of New Robust Procedures for the determination of maximum and minimum dry densities of sand. Proc 4 th Inter. Symp. On Frontiers in Offshore Geotechnics ISFOG

Le, V. H., and Rackwitz, F. (2020). A New Cyclic Simple Shear Test Procedure with Multidirectional Loading, *Geotechnical Testing Journal*, 43: 275-86

Peralta, P., Ballard, J.C., Rattley, M. and Erbrich, C.E., 2017, January. Dynamic and Cyclic Pile-Soil Response Curves for Monopile Design. *Offshore Site Investigation Geotechnics 8th International Conference Proceeding*

Richards, I. A., Byrne, B. W., and Houlsby, G. T. (2020). Monopile rotation under complex cyclic lateral loading in sand, *Géotechnique*, 70: 916-3